

Effect of Tungsten on the Thermal Hysteresis in the Resistivity of Vanadium Dioxide Films

O. Ya. Berezina^{a, *}, P. P. Boriskov^{a, **}, E. A. Tutov^b, V. P. Zlomanov^c, and N. A. Avdeev^a

^a *Petrozavodsk State University, Petrozavodsk, Karelia, 185910 Russia*

^b *Voronezh State Technical University, Voronezh, 394006 Russia*

^c *Moscow State University, Moscow, 119991 Russia*

**e-mail: berezina@petrsu.ru*

***e-mail: boriskov@petrsu.ru*

Received February 21, 2022; revised April 18, 2022; accepted April 19, 2022

Abstract—We analyze the effect of tungsten doping of sol–gel derived polycrystalline vanadium dioxide films on the temperature dependence of their resistivity across the metal–semiconductor transition. Experimental resistivity hysteresis data demonstrate that, with increasing doping level, the phase transition temperature of the films decreases, their hysteresis loop extends over a broader temperature range, and their resistivity jump drops. We have constructed coercive temperature distribution functions and compared them with size distributions of crystalline grains in the undoped and doped films. The results lead us to conclude that tungsten doping of vanadium dioxide has no effect (at least up to 6 at % W) on structure formation in polycrystalline films. The observed changes in phase transition parameters upon doping are, most likely, caused by the increase in donor defect density and the large scatter in dopant concentration in individual grains.

Keywords: metal–semiconductor phase transition, doping, coercive temperature method, sol–gel method

DOI: 10.1134/S0020168522070056

INTRODUCTION

The best known oxide material undergoing a metal–semiconductor transition (MST) is vanadium dioxide, which has been the subject of an enormous number of reports over the last six decades. The MST temperature of bulk VO₂ ($t_t \sim 68^\circ\text{C}$) is not far from room temperature, and the conductivity jump accompanying its phase transition is several orders of magnitude (up to 10^5). For a number of practical applications, such as “smart” windows [1] and optical limiters [2], it is desirable to lower the temperature t_t and reduce the width of the corresponding hysteresis loop. Note that the width of the MST hysteresis loop (first-order phase transition) is 1–3°C in the case of bulk crystals and much larger (up to 20°C) in the case of thin-film polycrystalline structures. At present, vanadium dioxide and VO₂-based compounds are typically prepared in the form of not only films [3] but also powders [4], nanorods [5], and nanofibers [6].

Researchers’ interest in vanadium dioxide and VO₂-based interstitial compounds is aroused by their thermodynamic stability and by the facts that they are relatively easy to synthesize and that their phase transition occurs near room temperature, which opens up a wide range of various practical applications. Exam-

ples include thermochromic smart coatings and relaxation oscillators as elements of oscillatory neural network [7–9]. In a number of studies, VO₂ was proposed as a material for chemisorption gas sensors for hydrogen [10] and ethanol vapor [11, 12]. Besides, it is potentially attractive for designing materials of electrochemical devices [13].

The incorporation of metals into the structure of vanadium dioxide can both raise its MST temperature (Cr and Fe) and lower it (Nb, W, and Mo) [14]. In a previous study, Berezina et al. [15] for the first time doped vanadium dioxide with tungsten via a sol–gel process. This way of doping offers the advantage of simple technology in combination with an acceptable degree of homogeneity and stoichiometry of the resultant films. In this work, the coercive temperature method is used for detailed analysis of the thermal hysteresis in the resistivity of sol–gel derived VO₂ films under MST conditions at various tungsten doping levels.

THEORETICAL ANALYSIS

Analysis of MST hysteresis effects in VO₂ [2, 16, 17] shows that hysteresis in polycrystalline films depends significantly on two parameters: crystallite (grain) size and stoichiometry (relationship between the vana-

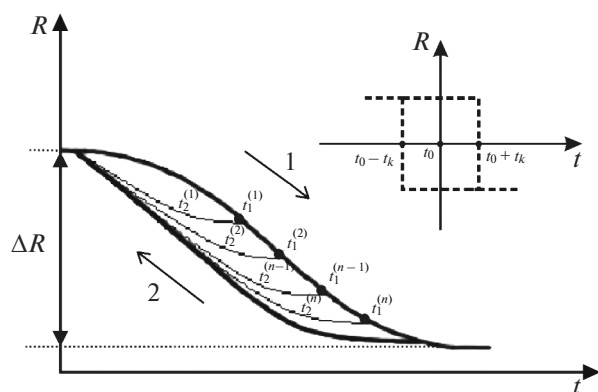


Fig. 1. MST hysteresis loops as functions of the parameter of the medium R and temperature t for a polycrystalline sample: the thick line represents the full hysteresis loop, with its forward (arrow 1) and reverse (arrow 2) portions; $t_1^{(1)}, t_1^{(2)} \dots t_1^{(n-1)}, t_1^{(n)}$ are the initial temperatures of partial loops ((1, 2 ... $n - 1, n$)); $t_2^{(1)}, t_2^{(2)} \dots t_2^{(n-1)}, t_2^{(n)}$ are current temperatures in the partial hysteresis loops; and ΔR is the total change in the parameter of the medium. Inset: square hysteresis loop for a monocrystallite.

dium and oxygen concentrations, which determines oxygen vacancy concentration) of the films. The smaller the average crystallite size in films, the broader their hysteresis loop [17]. On the other hand, the higher is the concentration of oxygen vacancies produced in VO_2 films, for example, by electron irradiation [16], the lower is the MST temperature.

To study MST hysteresis phenomena in vanadium dioxide, Lanskaya et al. [18] proposed an approach similar to analysis of a technical magnetization curve in ferromagnets, developed by Preisach [19] as early as 1935. This approach (coercive temperature method) assumes that there is a parameter of the medium, R , that depends on the phase transition and is a function of two variables: coercive temperature t_c and average (or thermodynamic) temperature t_0 . The temperature t_c is determined by the grain number–hysteresis loop width (Δt) distribution of individual grains (so-called partial distributions). Thus, t_c correlates with the grain size distribution. The temperature t_0 is responsible for the grain distribution with respect to the phase equilibrium temperature and depends on the stoichiometric composition of the grains.

The temperatures t_c and t_0 are the easiest to determine in the case of hysteresis of an individual monocrystallite, which has a square loop with a central (middle) temperature t_0 and the temperatures of its vertical portions $t_0 + t_c$ (heating) and $t_0 - t_c$ (cooling) (Fig. 1, inset); that is, the width of such a loop is $\Delta t = 2t_c$. The simplified analytical approach used by

Lanskaya et al. [18] assumes that a grain in a polycrystalline film consists of a set of such domains (microregions) with square hysteresis loops distributed with respect to t_c and t_0 . Hysteresis in a polycrystalline film, characterized by the distribution $F(t_0, t_c)$ of microregions with respect to the transition temperature and coercive temperature t_c , has a full loop with a forward (heating) and reverse (cooling) portions and a set of partial loops (Fig. 1). Each partial loop has its own initial temperature t_1 in the forward portion of the full loop and its own reverse portion (cooling) with a current temperature t_2 .

As shown by Lanskaya et al. [18], if the parameter of the medium is a linear function of the fraction of crystallites that converted to a new phase as a result of an MST, it will be a function of these two variables, $R(t_1, t_2)$, and the coercive function $F(t_0, t_c)$ will be defined as

$$F(t_c, t_0) = \frac{2}{\Delta R} \frac{\partial^2 R(t_1, t_2)}{\partial t_1 \partial t_2}, \quad t_0 = \frac{t_1 + t_2}{2}, \quad t_c = \frac{t_1 - t_2}{2}, \quad (1)$$

where ΔR is the total change in the parameter of the medium as a result of the MST (Fig. 1). Note that $F(t_0, t_c)$ has the meaning of the joint density of the distribution of the random variables t_0 and t_c .

Thus, construction of partial hysteresis loops allows one to determine the kind of the function $F(t_0, t_c)$. For this purpose, one fixes the initial temperature t_1 in the forward portion of the full loop in experiments (Fig. 1). Next, one measures the parameter of the medium (reflectivity of VO_2 film in Refs. [2, 16]) at a current temperature t_2 during cooling from the initial temperature t_1 up to the top point of the loop. A $\{R(t_1, t_2)\}$ set of partial loops and relation (1) are then used to calculate the distribution function $F(t_0, t_c)$.

The coercive temperature method encounters some difficulties in analysis of temperature dependences of electrical conductivity. In this case, the parameter of the medium (resistivity or conductivity) cannot be thought of as linear in the concentration of regions of some phase, in contrast to what was assumed for reflectivity, because inhomogeneity properties of the medium are essential. This becomes clear even from general considerations, given that even one conductive channel, which can be thought of as a chain of clusters (microregions) that transformed into a metallic phase, is sufficient for the current density in the film to be nonzero. Certainly, the probability of formation of such channels rises as the fraction of microregions having metallic conductivity increases, but the relation is not necessarily linear. In this case, the problem can be solved using percolation theory [20], which describes charge and mass transport phenomena in highly inhomogeneous media.

Consider a medium characterized by local electrical conductivity $\sigma(r)$ with a predetermined distribution law. In our case, this function can be thought to be highly inhomogeneous, as expressed by the relation [20]

$$\left| \frac{\sigma(r) - \langle \sigma(r) \rangle}{\langle \sigma(r) \rangle} \right| \gg 1, \quad (2)$$

where $\langle \sigma(r) \rangle$ is average conductivity. Indeed, under MST conditions it can take only two values, corresponding to a low-resistivity (metallic) and a high-resistivity (semiconducting) state of individual microregions, which differ by several orders of magnitude. It is worth noting, however, that severe inhomogeneity will be alleviated at the hysteresis edges, where regions in one of the two states will prevail.

The limiting (exponential) case of severe inhomogeneity is characterized by local conductivity

$$\sigma(r) = \sigma_0 \exp(-\xi(r)), \quad (3)$$

where σ_0 is the conductivity of the metallic state and $\xi(r)$ is a random variable characterizing the fraction of microregions in the metallic phase. Percolation theory [20] provides a certain critical value, ξ_c , below which ($\xi(r) < \xi_c$) no conductive channels are formed in the material. An important point is that this parameter is proportional to the fraction of microregions that converted to a new (low-resistivity) phase.

Similar conclusions can be drawn for resistivity: $\rho(r) = 1/\sigma(r)$. Then, under the assumption that the probability of the formation of low-resistivity microregions in the sample follows a uniform distribution law, $F(t_0, t_c)$ can be found using relation (1), where the parameter of the medium is the logarithm of average resistivity:

$$F(t_0, t_c) = \frac{2}{\ln\left(\frac{\rho_{\max}}{\rho_{\min}}\right)} \frac{\partial^2 (\ln \rho(t_1, t_2))}{\partial t_1 \partial t_2}, \quad (4)$$

where $t_0 = \frac{t_1 + t_2}{2}$ and $t_c = \frac{t_1 - t_2}{2}$.

In relation (4), the logarithm of the ratio of the average resistivities of VO₂ film in a fully semiconducting (ρ_{\max}) and a fully metallic (ρ_{\min}) state is the maximum change in the parameter of the medium (like ΔR in (1)).

Thus, constructing partial thermal hysteresis loops for the logarithm of the average resistivity or total resistance of films allows one to approximately determine the distribution function $F(t_0, t_c)$ in the same way as in the case of reflectivity [2, 16].

FILM GROWTH TECHNIQUE AND EXPERIMENTAL RESULTS

Vanadium dioxide films were produced using a liquid-phase sol-gel process [15]. First, we prepared an aqueous solution of vanadium pentoxide gel. V₂O₅ powder was melted and held at a temperature of 900°C for 1 h. Next, the melt was poured into distilled water at room temperature and stirred. To produce doped films, WO₃ powder was added to the V₂O₅ powder. After that, the resultant red brown gel-like solution was applied to a glass-ceramic substrate and dried for 24 h, until the formation of hydrous vanadium pentoxide (V₂O₅·*n*H₂O, *n* = 1.6–1.8) xerogel, in pure form or tungsten-doped.

To prepare vanadium dioxide by reducing the xerogel, the samples were vacuum-annealed at a temperature of 500 ± 20°C and residual vapor pressure below 0.13 Pa. Given that V₂O₅ and WO₃ differ in thermal stability, it is reasonable to expect that, at the annealing temperature used, the tungsten in WO₃ retains its oxidation state, whereas V₂O₅ is reduced to vanadium dioxide. As a result, we obtained polycrystalline films consisting of either undoped vanadium dioxide or doped one, presumably with the composition V_{1-y}W_yO₂, where *y* = 0.01–0.12. The effect of growth conditions on the composition and structure of the films was studied previously [15].

Figure 2 shows X-ray diffraction patterns of undoped and doped (12 at %) vanadium dioxide. It is seen that there is no shift of the diffraction peaks to within 0.1°; that is, the unit-cell parameters of the films remain unchanged. There are only changes in the intensity of some lines. The unit-cell parameters do not vary because, as a result of doping, W⁶⁺ ions substitute for some of the V⁴⁺ ions, and the ionic radii of V(IV) (0.073 nm) and W(VI) (0.072 nm) differ very little [17].

The resistivity of the vanadium oxide films was measured as a function of temperature by the four-probe technique in the temperature range from 50 to 400 K. For low-temperature measurements, the samples were placed in a cryorefrigerator.

The measurement results for the full hysteresis loops of the VO₂ films (Fig. 3) [15] demonstrate that the films containing up to 6 at % tungsten undergo an MST. The higher the dopant concentration, the lower the transition temperature *t_i*, the smaller the resistivity jump, the higher the conductivity in the high-resistivity state, and the lower that in the low-resistivity state. In the case of the films containing more than 6 at % W⁶⁺, no MST was detected in the temperature range 50–380 K (Fig. 3, curve 5).

Partial hysteresis loops were measured from the temperatures *t₁* and *t₂* in 1°C steps for the undoped and

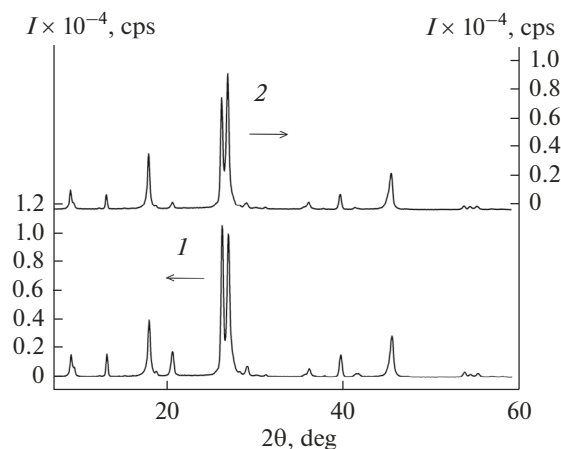


Fig. 2. X-ray diffraction patterns of (1) undoped and (2) tungsten-doped (12 at %) vanadium dioxide.

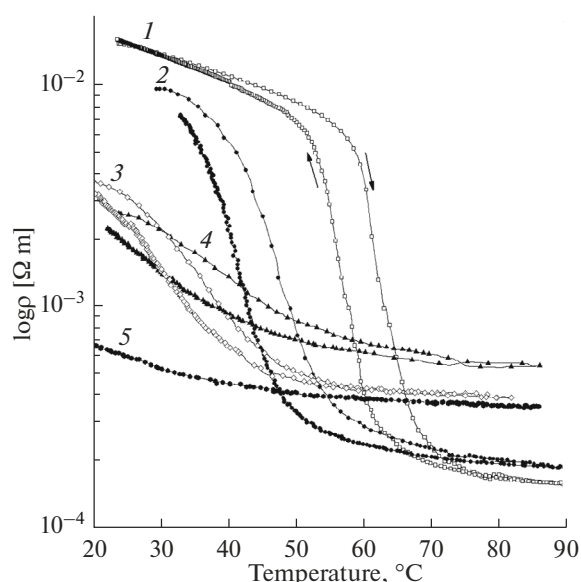


Fig. 3. Temperature dependences of resistivity for $V_{1-y}W_yO_{2\pm\delta}$ films according to Tutov et al. [11]: $y =$ (1) 0, (2) 0.016, (3) 0.03, (4) 0.06, and (5) 0.12.

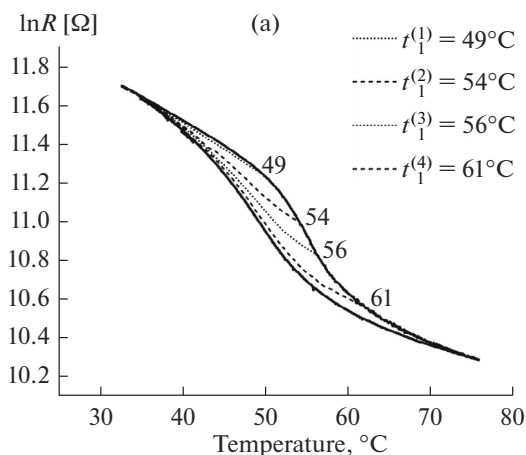


Fig. 4. Partial hysteresis loops of the logarithm of resistance for the (a) undoped and (b) 3 at % W^{6+} -doped vanadium dioxide films.

doped (3 at % W^{6+}) VO_2 films. Some of the partial loops are presented in Fig. 4. Using $\{\ln(R(t_1, t_2))\}$ experimental data sets and relation (4), we calculated the coercive function $F(t_0, t_c)$. The coercive temperature distribution density $f(t_c)$ can be found by integrating (summing) $F(t_0, t_c)$ with respect to t_0 :

$$f(t_c) \approx \sum_{t_0} F(t_0, t_c) = \sum_{t_0=t_{\min}}^{t_{\max}} F(t_0, t_c), \quad (5)$$

where t_{\max} and t_{\min} are the maximum and minimum temperatures of the full hysteresis loops, respectively. The $f(t_c)$ calculation results for the undoped and doped (3 at % W^{6+}) films are presented in Fig. 5.

Next, the surface of the samples (films) was examined by atomic force microscopy (AFM) on an SMM-2000 scanning electron microscope. AFM images (Fig. 6) were used to construct grain size distributions (Fig. 7) (relative number of grains as a function of their transverse size), which were essentially identical for the undoped and doped VO_2 samples. Since the undoped and doped films have identical grain size distributions on their surface (AFM data in Fig. 6) and identical unit-cell parameters (X-ray diffraction data in Fig. 2), it is reasonable to assume that they have identical grain size distributions in their bulk too.

CONCLUSIONS

Temperature-dependent electrical conductivity measurements, determination of the grain size distribution in VO_2 films, and calculation of coercive temperature functions for hysteresis lead us to the following conclusions:

1. The coercive temperature distribution function for the undoped sample (Fig. 5a) has two well-defined peaks and, in principle, correlates with the grain size distribution (Fig. 7, histogram 1). The peaks in the

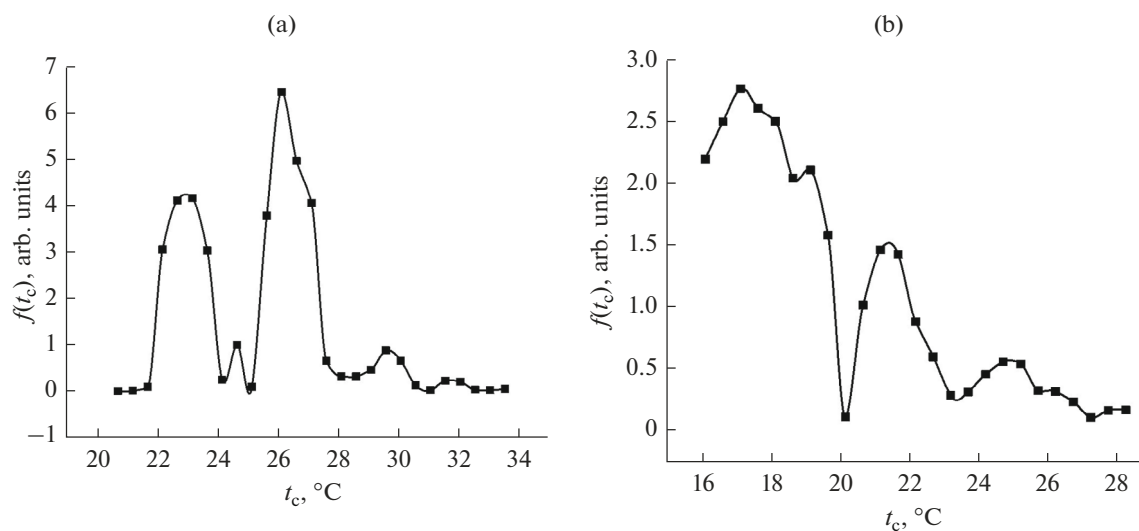


Fig. 5. Coercive functions $f(t_c)$ for the (a) undoped and (b) 3 at % W^{6+} -doped vanadium dioxide films.

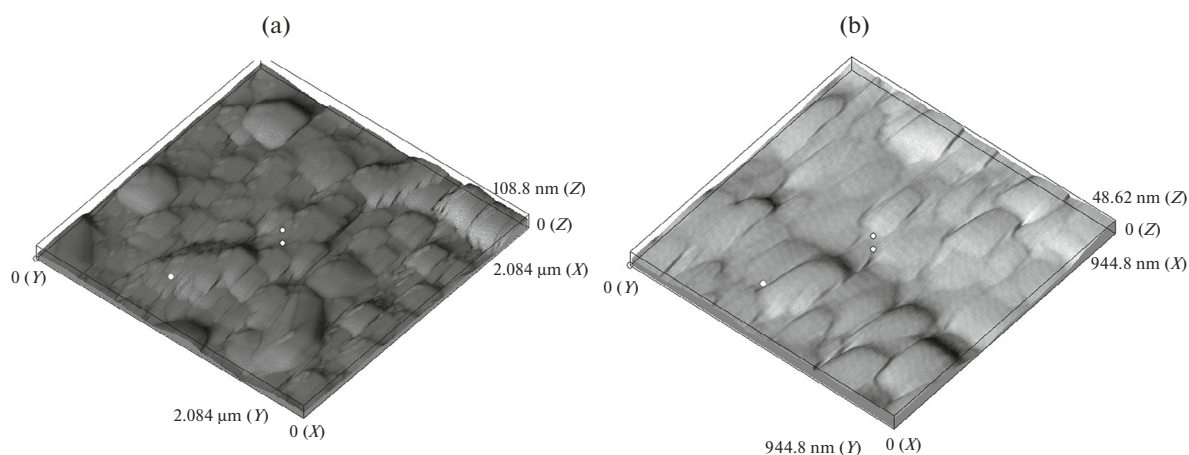


Fig. 6. AFM images of the surface of the (a) undoped and (b) 3 at % W^{6+} -doped sol-gel derived vanadium dioxide films.

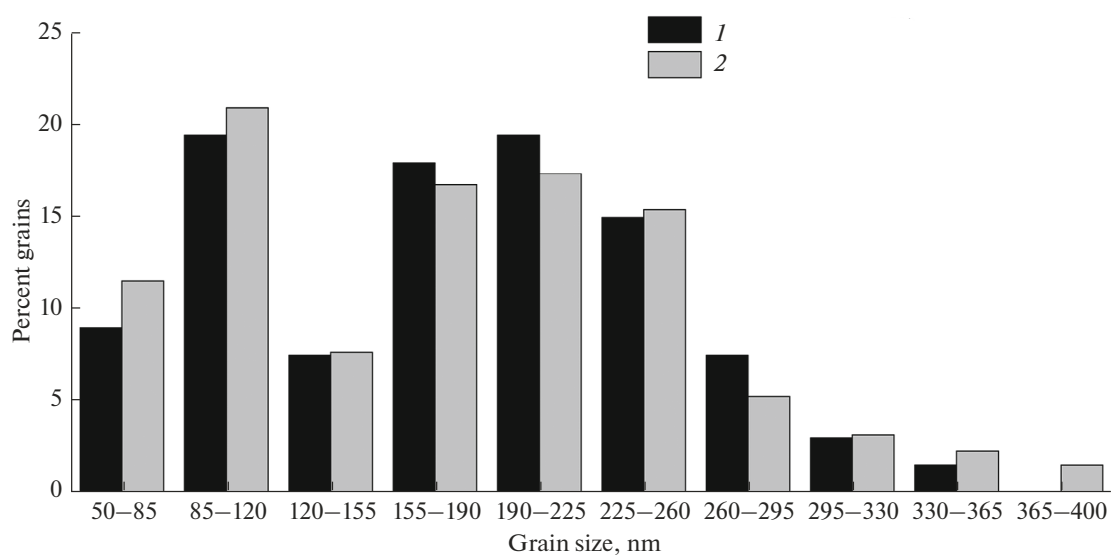


Fig. 7. Grain size distributions on the surface of the sol-gel derived vanadium dioxide films: (1) undoped sample and (2) 3 at % W^{6+} -doped sample.

coercive force distribution function of the doped film (Fig. 5b) are less well defined: the second (higher temperature) peak is considerably lower than the first (lower temperature) one, and both are severely broadened.

The observed large width of the coercive temperature function of the doped film attests to a more important role of deformation-induced distortion of the martensitic transition (in the form of broadening of partial loops of grains), which is a consequence of direct addition of the tungsten dopant. On the other hand, the identical grain size distributions in the undoped and doped vanadium dioxide films (Fig. 7) suggest that the W(VI) dopant has a weak effect on VO₂ grain growth. It may be that this is due to the identical growth conditions, the crystal-chemical similarity of V(IV) and W(VI) oxides, and the very small difference between the ionic radii of V(IV) (0.073 nm) and W(VI) (0.072 nm).

2. The electrical conductivity of the films rises with increasing dopant concentration owing to the substitution of W⁶⁺ ions for some V⁴⁺ centers. In the doped films, substitution of a W⁶⁺ ion for a V⁴⁺ ion should lead to the formation of two V³⁺ ions, which is dictated by the necessity to maintain electroneutrality; that is, donor defects are formed. The formation of donor defects leads to an increase in conductivity and a decrease in the MST temperature [16, 22].

3. We believe that the suppression of the MST in the heavily doped VO₂ films (above 6 at % tungsten) is caused by the severe inhomogeneity of the material, which has a large scatter in both grain size and dopant concentration in the grains because of the high doping level. In this case, the coercive temperature distribution function is very broad in terms of t_0 and t_c and, as a consequence, the forward and reverse portions of the MST hysteresis loop are very broad in temperature. Besides, raising the tungsten dopant concentration and, hence, the donor defect density considerably reduces the resistivity of the doped film in the semi-conducting state (ρ_{\max}), whereas the resistivity of the metallic phase (ρ_{\min}) exceeds that of the undoped film (Fig. 3, relation (4)). The resistivity jump decreases and disappears at a certain critical dopant concentration, transforming into a smooth function of temperature with no hysteresis; that is, there is no phase transition.

FUNDING

This work was supported by the Russian Federation Ministry of Science and Higher Education (state research target, theme no. 0752-2020-0007).

CONFLICT OF INTEREST

The authors declare that they have no conflicts of interest.

REFERENCES

- Seyfour, M. and Binions, R., Sol–gel approaches to thermochromic vanadium dioxide coating for smart glazing application, *Sol. Energy Mater. Sol. Cells*, 2017, vol. 159, pp. 52–65.
<https://doi.org/10.1016/j.solmat.2016.08.035>
- Klimov, V.A., Timofeeva, I.O., Khanin, S.D., Shadrin, E.B., Ilinskii, A.V., and Silva-Andrade, F., Hysteresis loop construction for the metal–semiconductor phase transition in vanadium dioxide films, *Tech. Phys.* 2002, vol. 47, no. 9, pp. 1134–1139.
<https://doi.org/10.1134/1.1508078>
- Makarevich, O.N., Ivanov, A.V., Gavrilov, A.I., et al., Effect of r -Al₂O₃ single-crystal substrate on growth of Ti_{1-x}V_xO₂ particles under hydrothermal conditions, *Russ. J. Inorg. Chem.*, 2020, vol. 65, no. 3, pp. 299–304.
<https://doi.org/10.1134/S0036023620030080>
- Nosikova, L.A., Baranchikov, A.E., Yapryntsev, A.D., et al., Selective hydrothermal synthesis of [(CH₃)₂NH₂]V₃O₇, VO₂(D), and V₂O₃ in the presence of *N,N*-dimethylformamide, *Russ. J. Inorg. Chem.*, 2020, vol. 65, no. 4, pp. 488–494.
<https://doi.org/10.1134/S0036023620040142>
- Volkov, V.L., Zakharova, G.S., Volkova, E.G., et al., Titanium-doped vanadium oxide nanorods, *Russ. J. Inorg. Chem.*, 2006, vol. 51, no. 6, pp. 847–851.
<https://doi.org/10.1134/S0036023606060015>
- Berezina, O.Ya., Kolobova, E.N., Krivoshepov, N.V., Markova, N.P., Pergament, A.L., Yakovleva, D.S., and Zlomanov, V.P., Vanadium oxide nanofibers: synthesis and research on functional properties, *Micro Nanosyst.*, 2020, vol. 12, no. 2, pp. 1–7.
<https://doi.org/10.2174/1876402911666190806104117>
- Pergament, A.L., Stefanovich, G.B., and Velichko, A.A., Oxide electronics and vanadium dioxide perspective: a review, *J. Sel. Top. Nano Electron. Comput.*, 2013, vol. 1, no. 1, pp. 24–43.
<https://doi.org/10.15393/j8.art.2013.3002>
- Zhang, Z., Gao, Y., Chen, Z., Du, J., Cao, C., Kang, L., and Luo, H., Thermochromic VO₂ thin films: solution-based processing, improved optical properties, and lowered phase transformation temperature, *Langmuir*, 2010, vol. 26, no. 13, pp. 10738–10744.
<https://doi.org/10.1021/la100515k>
- Velichko, A., Belyaev, M., Putrolainen, V., Pergament, A., and Perminov, V., Switching dynamics of single and coupled VO₂-based oscillators as elements of neural networks, *Int. J. Mod. Phys. B*, 2016, vol. 30, no. 2, paper 165026.
<https://doi.org/10.1142/s0217979216502611>
- Strelcov, E., Lilach, Y., and Kolmakov, A., Gas sensor based on metal–insulator transition in VO₂ nanowire thermistor, *Nano Lett.*, 2009, vol. 9, no. 6, pp. 2322–2326.
<https://doi.org/10.1021/nl900676n>
- Tutov, E.A., Manannikov, A.V., Al-Khafaji, H.I., and Zlomanov, V.P., Surface and bulk conductivity of vana-

- dium dioxide, *Tech. Phys.*, 2017, vol. 87, pp. 390–394. <https://doi.org/10.1134/S1063784217030252>
12. Tutov, E.A. and Zlomanov, V.P., Effect of chemisorption of donor and acceptor gases on the semiconductor–metal phase transition in vanadium dioxide films, *Phys. Solid State*, 2013, vol. 55, no. 11, pp. 2351–2354. <https://doi.org/10.1134/S1063783413110280>
 13. Armer, C.F., Yeoh, J.S., Xu Lib, and Lowe, A., Electrospun vanadium-based oxides as electrode materials, *J. Power Sources*, 2018, vol. 395, pp. 414–429. <https://doi.org/10.1016/j.jpowsour.2018.05.076>
 14. Bugaev, A.A., Zakharchenya, B.P., and Chudnovskii, F.A., *Fazovyi perekhod metal–poluprovodnik i ego primeneniye* (Metal–Semiconductor Transition and Its Applications), Leningrad: Nauka, 1979.
 15. Berezina, O.Ya., Velichko, A.A., Lugovskaya, L.A., Pergament, A.L., and Stefanovich, G.B., Metal–semiconductor transition in nonstoichiometric vanadium dioxide films, *Inorg. Mater.*, 2007, vol. 43, no. 5, pp. 505–511. <https://doi.org/10.1134/S0020168507050123>
 16. Shadrin, E.B. and Il'inskii, A.V., On the nature of metal–semiconductor phase transition in vanadium dioxide, *Phys. Solid State*, 2000, vol. 42, no. 6, pp. 1126–1133. <https://doi.org/10.1134/1.1131328>
 17. Aliev, R.A. and Klimov, V.A., Effect of synthesis conditions on the metal–semiconductor phase transition in vanadium dioxide thin films, *Phys. Solid State*, 2004, vol. 46, no. 3, pp. 532–536. <https://doi.org/10.1134/1.1687874>
 18. Lanskaya, T.G., Merkulov, I.A., and Chudnovskii, F.A., Hysteretic phenomena accompanying the metal–semiconductor phase transition of vanadium oxides, *Fiz. Tverd. Tela* (Leningrad), 1978, vol. 20, no. 2, pp. 336–342.
 19. Preisach, F., Über die magnetische Nachwirkung, *Z. Phys.*, 1935, vol. 94, nos. 5–6, pp. 277–302.
 20. Shklovskii, B.I. and Efros, A.L., Percolation theory and conduction in highly inhomogeneous media, *Usp. Fiz. Nauk*, 1975, vol. 117, no. 3, pp. 401–435.
 21. Tret'yakov, Yu.D., *Neorganicheskaya khimiya* (Inorganic Chemistry), vol. 3: *Khimiya perekhodnykh elementov* (Chemistry of Transition Elements), Moscow: Akademiya, 2007, issue 1.
 22. Castro, R.A., Ilinskii, A.V., Smirnova, L.M., Pashkevich, M.E., and Shadrin, E.B., Ellipsometry of nanocrystalline VO₂, VO₂:Mg, and VO₂:Ge films, *Fiz. Tverd. Tela*, 2021, vol. 63, no. 12, pp. 2210–2216. <https://doi.org/10.21883/FTT.2021.12.51686.184a>

Translated by O. Tsarev